Int. J. Solids Structures Vol. 22, No. 11, pp. 1307–1323, 1986
Printed in Great Britain.

0020-7683/86 $3.00 + .00
Pergamon Journals Ltd.

ON THE STABILITY OF CYLINDRICAL PNEUMATICS SUBJECTED TO SYMMETRIC LINE AND LIQUID LOADING

W. SZYSZKOWSKI and P. G. GLOCKNER
Department of Mechanical Engineering, University of Calgary, Calgary, Alberta, Canada

(*Received* 31 *January* 1985)

Abstract—The finite deflection and stability behaviour of cylindrical inextensible inflatables subjected to the weight of a ponding medium accumulating in a symmetric depression around the apex caused by a uniform symmetric line load or an initial depression/imperfection is treated using geometrically 'exact' equations. The vertical and lateral stability of these structures is analyzed by superimposing infinitesimal lateral disturbances onto the finite symmetric vertical displacement field. Separating the derived equations into symmetric and antisymmetric parts, the conditions for vertical and lateral stability are established. Numerical results indicate the various stability domains for these structures. A simple expression allowing estimation of the critical line load value for vertical instability, the prevailing mode of failure for such membranes, is established. The magnitude of initial depressions leading to ponding collapse is also established.

1. INTRODUCTION

Even relatively small and apparently 'safe' concentrated loads may become dangerous when applied to pneumatic structures in the presence of a ponding medium accumulating in the depression(s) caused by such loads. Such load conditions exist under a variety of environmental conditions including heavy rain or snow falls. Whether such load conditions lead to total failure of the membrane depends on the relation between rate of increase of the depression and the growth rate of the dead weight of the pond which, in turn, depend on the geometry of the structure, the internal over pressure and other parameters. Unlike other types of failure of such inflatables, which generally are signalled by internal pressure drop, the types of failure caused by this load configuration, referred to as 'ponding instability', is usually not accompanied by any drastic change in internal pressure and can therefore occur quite suddenly and without any prior warning.

Such concentrated or line loads when applied to membranes produce very large deflections necessitating a geometrically non-linear analysis. The pressure load due to the accumulating ponding medium is deflection dependent and thus nonconservative thereby adding to the complexity of the analysis.

Numerical solutions for the non-linear deflection behaviour of membranes subjected to conservative loadings, using finite element techniques, were recently reported[1, 2]. These solutions, however, tend to be costly and are normally not very convenient in reaching general conclusions. The non-linear ponding-instability problem for spherical membranes was discussed in Ref. [3] in which only axisymmetric finite deflections were admitted and which extended a previous analysis[4]. An analysis of the analogous ponding instability problem for cylindrical inflatables, restricted to small symmetric deflections, 'shallow' ponds and low-profile structures was presented in Ref. [5].

This paper extends the analysis given in Ref. [5] by studying both vertical and lateral instability of such structures subjected to symmetric line and liquid loading. The analysis admits non-shallow ponds and large vertical deflections. Although elasticity of the membranes could easily be included, this paper is restricted to inextensible membranes. An 'exact' analysis of the vertical and lateral instability of such cylindrical inflatables subjected only to a symmetric line load applied at the apex was given in Ref. [6] where it was shown that lateral instability is the governing mode of failure for very high profile structures and where the buckling behaviour was easily separated into modes associated with the symmetric and antisymmetric deformed states. Such a decomposition of the buckling modes is shown to be possible also for the 'ponding' case but is naturally more complex. The

relations defining the finite symmetric deflections and conditions for vertical or lateral instability are derived as separate sets of equations, one for each of vertical and lateral instability, including elliptic integrals. This paper also treats the problem of initial depression/imperfection leading to the 'liquid-loading only' case.

Numerical results obtained from the analysis permit determination of either the 'safe' limit value for symmetric uniform active line loads or the critical magnitude of initial deflections/depressions caused by 'passive' line loads due to tie-downs. These critical load/depression magnitudes define the limits below which the membrane is safe against lateral and vertical instability when subjected to such 'ponding' loads. The results also permit the formulation of simple closed-form expressions for the critical values of the line load and the initial depression, expressions which may prove useful in the design of such structures or for associated codes and specifications.

2. THE PONDING PHENOMENON

Let us examine the stability and safety of a cylindrical inflatable membrane by following the deflection/accumulation process of such a structure while subjected to a symmetric uniform line load applied at the apex (Figs 1(a) and (b), Phase 1) in the presence of a ponding medium accumulating in the depression caused by the load. First treat the case of an 'active' line load, W, the magnitude of which remains constant during deformation (Fig. 1(a)). Clearly, the deflection under the load as well as the volume/weight of the accumulating ponding medium will be increasing initially (Fig. 1(a), Phase 2). Depending on the combination of line load magnitude, internal pressure, initial geometry and ponding medium density, one of two scenarios in the symmetric load/deflection behaviour of the structure will develop: (i) a state where the ponding medium fills the depression to capacity (Fig. 1(a), Phase 3) with no further ponding or increase in deflection possible and thereby leading to a stable equilibrium configuration, (ii) a state in which the ponding medium does

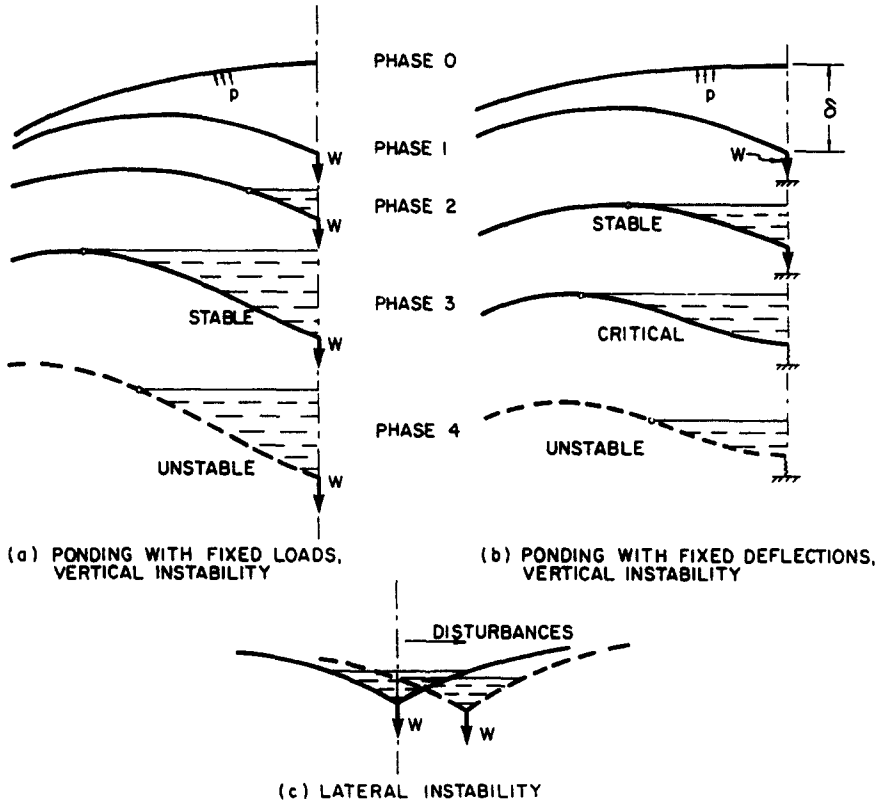

Fig. 1. Concepts on ponding instability.

not fill the depression to capacity (Fig. 1(a), Phase 4) and consequently the ponding process is continuing, with increasing deflections leading to failure. This combination of parameters thus clearly represents a vertically unstable configuration. The maximum value of this line load, W, for which the completely filled stable configuration is possible for a given initial geometry, internal pressure and ponding medium density will be referred to as the critical vertical load, W_v. Determination of this critical load, as a function of these parameters, is one objective of this analysis.

Next let us treat the case of a symmetric initial depression/imperfection caused by a 'tie-down' line load as shown in Fig. 1(b), Phase 1. Such a line load, which is, of course deflection dependent, will be referred to as a 'passive' load. The magnitude, W, of such a passive line load will decrease as the ponding medium accumulates in the depression and thereby relieves some of the tension in the tie-down cables. Again, two possible scenarios may develop as ponding medium accumulates in the depression. (i) A state where the ponding medium fills the depression to capacity and the tension in the tie-down cables is still nonzero (Fig. 1(b), Phase 2). This is clearly, again, a vertically stable configuration, since the ponding process terminates. (ii) A state in which the tension in the tie-down cables goes to zero before the depression is completely filled (Fig. 1(b), Phase 4) thereby leading to a vertically unstable configuration similar to the one discussed above. The 'critical' configuration corresponds to the case when the tension in the tie-down cables vanishes at the same time as the depression is filled to capacity (Fig. 1(b), Phase 3). The magnitude of this depression, δ, is referred to as the 'critical imperfection' the determination of which is a second objective of this paper.

In addition to vertical instability, such a membrane might fail laterally. Clearly, lateral instability is of interest only for vertically stable configurations. Consequently, in our lateral instability considerations we will deal only with configurations in which the depression is completely filled with an accumulating ponding medium (Fig. 1(c)). Lateral instability is established by examining the conditions under which an adjacent asymmetric disturbed state can exist. The maximum value of the line load for which such critical configurations are laterally stable is designated as W_L. The smaller of W_v and W_L is the 'safe line load limit' to which such cylindrical inflatables can be subjected while under the action of the above described environmental conditions.

3. GOVERNING EQUATIONS FOR GENERALLY DEFORMED STATE

In discussing the lateral stability of cylindrical inflatables, the general unsymmetric deformation field, as shown in Fig. 2, is required. Consider the deformed cross-section of such a structure when subjected to a uniform line load, W, with eccentricity ϕ_0 in the presence of an accumulating ponding medium of density γ (see Fig. 2). This deformed cross-section consists of two circular arcs of radii R_i ($i = 1, 2$) and two segments, L_i, in the pond region, where in addition to the internal pressure, p, there is also an external pressure due to the ponding medium. In this work we assume the medium to be a liquid and therefore, the magnitude of the pressure is hydrostatic. Friction is, thus, absent; in addition we assume the membrane weight to be negligible and consequently the circumferential stress resultant, S, is constant along the two portions of the membrane to either side of the line load, these constant values being $S_1 = pR_1$ and $S_2 = pR_2$, respectively.

For an element of the membrane in the ponding region, there is an equation of equilibrium normal to the deflected shape to be satisfied and written as

$$S = (\gamma \cdot h - p)\frac{dL}{d\alpha} \tag{1}$$

which when rewritten in terms of an orthogonal coordinate system, h, η (see Fig. 2) becomes

$$\frac{d^2\bar{h}}{d\bar{\eta}^2} - \left[\left(\frac{d\bar{h}}{d\bar{\eta}}\right)^2 + 1\right]^{3/2} \cdot \left(\frac{1-\bar{\gamma}\bar{h}}{\bar{S}}\right) = 0. \tag{2}$$

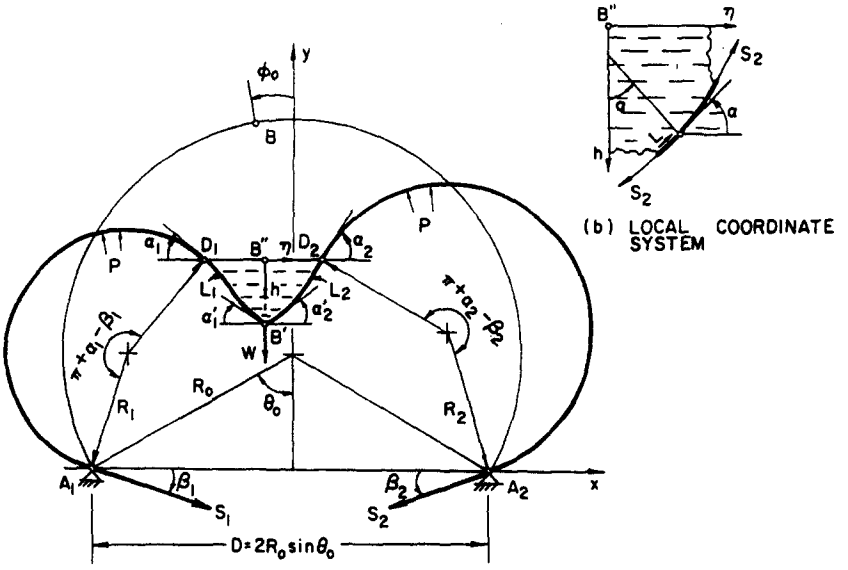

Fig. 2. Unsymmetrically deformed cross-section.

where $\bar{h} = h/R_0$; $\bar{\eta} = \eta/R_0$; $\bar{\gamma} = \gamma R_0/p$; $\bar{S} = S/pR_0$. For shallow ponds for which $|d\bar{h}/d\bar{\eta}| \ll 1.0$, eqn (2) can be linearized and a solution to such an approximate equation written in the form

$$\bar{h} = A \sin(r\bar{\eta}) + B \cos(r\bar{\eta}) + \frac{1}{\bar{\gamma}} \tag{3}$$

where $r^2 = \bar{\gamma}/\bar{S}$ and A, B denote integration constants. This result was used in Refs [5, 7] to study the vertical ('ponding') stability of such membranes while undergoing relatively small deflections.

The non-linear equation, eqn (2), has a form similar to that of the governing equation for finite post-buckling behaviour of an elastic column[8] which, as is known, is given in terms of elliptic integrals. In the present problem it is convenient to introduce the coordinate system, h, α (see Fig. 2(b)) in terms of which eqn (2) is recast as

$$\frac{d\bar{h}}{d\alpha} = \frac{\bar{S} \sin\alpha}{1 - \bar{\gamma}\bar{h}} \tag{4}$$

which can be integrated to obtain

$$\bar{h} - \frac{\bar{\gamma}}{2}\bar{h}^2 = -\bar{S}\cos\alpha + C \tag{5}$$

where C is an integration constant to be evaluated. Since $\bar{S}$ is $\bar{S}_1$ and $\bar{S}_2$ for the two segments, L_i, the two portions of the membrane in the ponding region will be defined by two separate functions, each in the form of eqn (5). Choosing the origin for $\bar{h}$ to be at the level of the pond surface one establishes

$$C_i = \bar{S}_i \cos\alpha_i$$

with which one finally rewrites eqn (5) as

$$\cos\alpha = \cos\alpha_i - \frac{\bar{h}}{\bar{S}_i}\left(1 - \frac{\bar{\gamma}\bar{h}}{2}\right), \qquad (i = 1, 2). \tag{6}$$

In the orthogonal coordinate system, $\bar{h}, \bar{\eta}$, the second coordinate can now be expressed in the form

$$\bar{\eta}(\bar{h}) = \bar{\eta}_i(0) \pm \int_0^{\bar{h}} \frac{\mathrm{d}\bar{h}}{\tan\alpha} = \bar{\eta}_i(0) \pm \int_0^{\bar{h}} \frac{\cos\alpha_i - \dfrac{\bar{h}}{\bar{S}_i}\left(1 - \dfrac{\bar{\gamma}\bar{h}^2}{2}\right)}{\sqrt{\left\{1 - \left[\cos\alpha_i - \dfrac{\bar{h}}{\bar{S}_i}\left(1 - \dfrac{\bar{\gamma}\bar{h}^2}{2}\right)\right]^2\right\}}} \mathrm{d}\bar{h} \tag{7}$$

where the '+' and '−' correspond to $i = 1$ and 2, respectively. Substituting for $\bar{h}$ the expression

$$\bar{h} = \frac{1}{\bar{\gamma}}(1 - \sqrt{B_i}\cos\phi); \qquad B_i = 1 + (1 - \cos\alpha_i)2\bar{S}_i\bar{\gamma} \tag{8a,b}$$

into eqn (7), one obtains a form containing elliptic integrals of the first and second kind, as

$$\bar{\eta}(\phi) = \bar{\eta}_i \pm \sqrt{\left(\frac{\bar{S}_i}{\bar{\gamma}}\right)}\left[2\int_{\phi_i^D}^{\phi} \sqrt{(1 - k_i^2\sin^2\phi)}\,\mathrm{d}\phi - \int_{\phi_i^D}^{\phi} \frac{\mathrm{d}\phi}{\sqrt{(1 - k_i^2\sin^2\phi)}}\right] \tag{9}$$

in which $k_i^2 = B_i/(4\bar{S}_i\bar{\gamma})$; $\cos\phi_i^D = 1/\sqrt{B_i}$ and where ϕ_i^D denote the values of ϕ corresponding to points D_i ($i = 1, 2$). Equations (6) and (7) define the shape and all associated parameters for the submerged portion of the membrane provided α_i, α_i' and $\bar{S}_i$ are known for each segment, L_i. For example, the depth of the pond, $\bar{h}_B$, can be established from the equation

$$\bar{h}_B\left(1 - \frac{\bar{\gamma}\bar{h}_B}{2}\right) = \bar{S}_i(\cos\alpha_i - \cos\alpha_i'); \qquad i = 1, 2 \tag{10}$$

while the lengths of the segments, L_i, are determined as

$$\bar{L}_i = \int_0^{\bar{h}_B} \frac{\mathrm{d}\bar{h}}{\sin\alpha} = \sqrt{\left(\frac{\bar{S}_i}{\bar{\gamma}}\right)} \int_{\phi_i^D}^{\phi_i^B} \frac{\mathrm{d}\phi}{\sqrt{(1 - k_i^2\sin^2\phi)}} \tag{11}$$

where $\cos\phi_i^B = (1 - \bar{\gamma}\bar{h}_B)/\sqrt{B_i}$ and $\bar{L}_i = L_i/R_0$. The total weight of the pond, Q, is expressed as

$$\bar{Q} = \frac{Q}{pR_0} = \bar{S}_1\sin\alpha_1 + \bar{S}_2\sin\alpha_2 - \bar{\eta}_1 + \bar{\eta}_2 - \bar{W} \tag{12}$$

in which $\bar{\eta}_i$ can be found from eqn (9) by substituting $\phi = \phi_i^B$ at which point $\bar{h} = \bar{h}_B$ and $\bar{\eta}(\phi_i^B) = 0$.

When the expression is filled to capacity, one of the angles α_i, say α_1, is zero. Therefore $B_1 = 1 \rightarrow \phi_1^D = 0$; also

$$\bar{L}_1 = \frac{1}{2k_1\bar{\gamma}}\int_0^{\phi_1^D} \frac{\mathrm{d}\phi}{\sqrt{(1 - k_1^2\sin^2\phi)}} = \frac{1}{2k_1\bar{\gamma}} F(k_1, \phi_1^D) \tag{13a}$$

$$\bar{\eta}_1 = -\frac{1}{k_1\bar{\gamma}}\left[\int_0^{\phi_1^D} \sqrt{(1 - k_1^2\sin^2\phi)}\,\mathrm{d}\phi - \frac{1}{2}\int_0^{\phi_1^D} \frac{\mathrm{d}\phi}{\sqrt{(1 - k_1^2\sin^2\phi)}}\right]$$

$$= -\frac{1}{k_1\bar{\gamma}}[E(k_1, \phi_1^D) - \tfrac{1}{2}F(k_1, \phi_1^D)] \tag{13b}$$

where $F(k_1, \phi_1^D)$ and $E(k_1, \phi_1^D)$ are elliptic functions of the first and second kinds, respectively.

If, in addition, α_1' is also zero, as is the case for the loading state depicted in Fig. 1(b),

Phase 3, then $\bar{h}_B = 2/\bar{\gamma}$, $\phi_1^B = \pi$ and eqns (13) become

$$\bar{L}_1 = \frac{1}{k_1\bar{\gamma}} F(k_1, \pi/2)$$
$$\bar{\eta}_1 = -\frac{1}{k_1\bar{\gamma}} [2E(k_1, \pi/2) - F(k_1, \pi/2)] \tag{14a,b}$$

in which now the so-called 'complete' elliptic functions appear. Well-known general properties of these elliptic functions will be useful in our further considerations.

Having defined the deformed shape of the membrane we next consider the static and geometric conditions of the problem by writing (see Fig. 1):

(i) local equilibrium equations at point B

$$\bar{S}_1 \cos\alpha_1' - \bar{S}_2 \cos\alpha_2' = 0$$
$$\bar{S}_1 \sin\alpha_1' + \bar{S}_2 \sin\alpha_2' = \bar{W}; \tag{15a,b}$$

(ii) overall equilibrium equations for the membrane

$$\bar{S}_1 \cos\beta_1 - \bar{S}_2 \cos\beta_2 = 0$$
$$\bar{S}_1 \sin\beta_1 + \bar{S}_2 \sin\beta_2 = 2\sin\theta_0 - \bar{W} - \bar{Q} \tag{16a,b}$$

where θ_0 is the central half angle of the membrane and β_i denote slopes of the membrane at the supports;

(iii) geometric relations (compatibility) incorporating inextensibility

$$(\pi + \alpha_1 - \beta_1)\bar{R}_1 + \bar{L}_1 = \pi - \theta_0 + \phi_0$$
$$(\pi + \alpha_2 - \beta_2)\bar{R}_2 + \bar{L}_2 = \pi - \theta_0 - \phi_0 \tag{17a,b}$$

where $\bar{R}_i = R_i/R_0$. For the circular portions of the membrane, clearly $S_i = pR_i$ or in dimensionless variables $\bar{S}_i = \bar{R}_i$. The eight equations, eqns (10), (15)–(17) define the deformed geometry of the membrane in terms of the eight variables, $\alpha_i, \alpha_i', \beta_i$ and $\bar{R}_i$ $(i = 1, 2)$ for a given line load value, W and a given pond parameter, Q or the depth, $\bar{h}_B$, or some other variable associated with the deformed pond geometry. Symbolically, these equations are written in the form

$$G[V, q(V)] = 0 \tag{18}$$

where G denotes non-linear operations, described by eqns (10), (15)–(17), on the geometric variables of the deformed state, denoted here by the vector V, and on the external load function, q, which in our case is also deflection dependent. The deflections of the membrane can be determined by rearranging this equation in the form

$$V = g(q). \tag{19}$$

Due to the multivaluedness of the trigonometric functions appearing in the equations, severe convergence problems are encountered when attempting to solve eqn (19) numerically. For a shallow pond, some details of such an analysis and the related difficulties encountered are discussed in Ref. [7].

4. STATIC AND STABILITY ANALYSIS OF FINITE SYMMETRIC DEFORMATION OF CYLINDRICAL MEMBRANES

In this paper we will deal with the case of a uniform line load, W, applied at the apex ($\phi_0 = 0$) in the presence of an accumulating ponding medium which fills the depression

caused by W completely. Thus, in the laterally disturbed state, the angles α_i take the values $\alpha_1 = 0$ and $\alpha_2 > 0$, or vice versa. The condition, $\alpha_1 = 0$, provides the additional specification which permits complete determination of the deflected shape in the ponding region.

For such initially symmetric loadings we obviously expect a symmetric mode of deformation. However, this mode may become unsymmetric due to lateral instability and associated lateral displacements. The analysis, therefore, proceeds by assuming that the deformation field consists of finite symmetric deflections with infinitesimal unsymmetric displacements superimposed on this field. The displacement field, V, for such a 'disturbed' state can be written as

$$V = \begin{bmatrix} \alpha_1 \\ \alpha_2 \\ \alpha_1' \\ \alpha_2' \\ \beta_1 \\ \beta_2 \\ \bar{R}_1 \\ \bar{R}_2 \end{bmatrix} = \begin{bmatrix} 0 \\ 0 \\ \alpha' \\ \alpha' \\ \beta \\ \beta \\ \bar{R} \\ \bar{R} \end{bmatrix} + \begin{bmatrix} 0 \\ \delta\alpha_2 \\ \delta\alpha_1' \\ \delta\alpha_2' \\ \delta\beta_1 \\ \delta\beta_2 \\ \delta\bar{R}_1 \\ \delta\bar{R}_2 \end{bmatrix} = \mathring{V} + \delta V \tag{20}$$

where $\mathring{V}(0, \alpha', \beta, \bar{R})$ are variables associated with the finite symmetric displacement field and $\delta V(0, \delta\alpha_2, \delta\alpha_1', \delta\alpha_2', \delta\beta_1, \delta\beta_2, \delta\bar{R}_1, \delta\bar{R}_2)$ represent infinitesimal disturbances. Note that during the 'disturbance' of the axisymmetric field, the line load is held constant, i.e. $\delta W = 0$, which leads to the determination of the extremum of W.

The disturbed state has to satisfy the governing equations, eqns (18), which when developed into a Taylor series with respect to the variations δV can be written in the form

$$G[V, q(V)] = G[\mathring{V}, q(\mathring{V})] + \left.\frac{\partial G}{\partial V}\right|_{V=\mathring{V}} \delta V = 0 \tag{21}$$

from which we obtain the following two relations

$$G[\mathring{V}, q(\mathring{V})] = 0 \tag{22}$$

$$\left.\frac{\partial G}{\partial V}\right|_{V=\mathring{V}} \delta V = 0 \tag{23}$$

defining the equilibrium of the finite symmetric and the neutral stability states of the structure, respectively.

After some algebra, eqn (22) can be rewritten in the form

$$(\pi - \theta_0 - \bar{L}) \sin\beta = (\pi - \beta)[\sin\theta_0 - \bar{\eta}] \tag{24a}$$

where

$$\bar{L} = \frac{1}{2k\bar{\gamma}} F(k, \phi^B); \qquad \cos\phi^B = 1 - \bar{\gamma}\bar{h}_B \tag{24b,c}$$

$$\bar{\eta} = \frac{1}{k\bar{\gamma}} [E(k, \phi^B) - \tfrac{1}{2}F(k, \phi^B)] \tag{24d}$$

$$k^2 = \frac{1}{4\bar{R}\bar{\gamma}} = \frac{1}{4\bar{\gamma}} \frac{\pi - \beta}{(\pi - \theta_0 - \bar{L})}. \tag{24e}$$

For given θ_0 and $\bar{\gamma}$ and an assumed value of $\bar{h}_B$, substitution of eqns (24b)–(24e) into eqn (24a) leads to an expression in terms of only one unknown, namely β, which can be solved and the value of β and all other parameters defining the deformed shape of the membrane determined; thus one obtains

$$\bar{R} = \frac{\pi - \theta_0 - \bar{L}}{\pi - \beta} \tag{25a}$$

$$\cos\alpha' = 1 - \frac{\bar{h}_B}{\bar{R}}\left(1 - \frac{\bar{\gamma}\bar{h}_B}{2}\right) \tag{25b}$$

$$\bar{W} = 2\bar{R}\sin\alpha' \tag{25c}$$

$$\bar{\delta}_B = 1 + \cos\theta_0 - \bar{R}(1+\cos\beta) + \bar{h}_B \tag{25d}$$

where $\bar{\delta}_B$ denotes the total central deflection of the membrane.

The equation defining the neutral stability of the system, eqn (23), becomes more tractable if the general field of disturbance, δV, is decomposed into two portions as

$$\delta V = \begin{bmatrix} 0 \\ \delta\alpha_2 \\ \delta\alpha_1' \\ \delta\alpha_2' \\ \delta\beta_1 \\ \delta\beta_2 \\ \delta\bar{R}_1 \\ \delta\bar{R}_2 \end{bmatrix} = \begin{bmatrix} 0 & 0 \\ 0 + \delta\alpha_a \\ \delta\alpha_s' + \delta\alpha_a' \\ \delta\alpha_s' - \delta\alpha_a' \\ \delta\beta_s + \delta\beta_a \\ \delta\beta_s - \delta\beta_a \\ \delta\bar{R}_s + \delta\bar{R}_a \\ \delta\bar{R}_s - \delta\bar{R}_a \end{bmatrix} = \delta V_s \pm \delta V_a \tag{26}$$

where the subscripts 's' and 'a' denote symmetric and antisymmetric disturbances, respectively. Note, however, that when $\delta V_a = 0$, the disturbance field, δV_s, is perfectly symmetric, while if $\delta V_s = 0$, the disturbances associated with δV_a are not exactly skew symmetric due to the presence of the component $\delta\alpha_a$ (see Fig. 3). As will be shown in the sequel, the modes related to these two kinds of disturbances are orthogonal, with the first one being symmetric and the second one, denoted by δV_a, being referred to here as 'antisymmetric'.

Substituting eqn (26) into eqns (15a) and (16a), we have

$$\begin{aligned} \delta\bar{R}_a\cos\alpha' - \bar{R}\sin\alpha'\,\delta\alpha_a' &= 0 \\ \delta\bar{R}_a\cos\beta - \bar{R}\sin\beta\,\delta\beta_a &= 0. \end{aligned} \tag{27a,b}$$

Analogously, from eqns (15b) and (16b) one obtains

$$\begin{aligned} \delta\bar{R}_s\sin\alpha' + \bar{R}\cos\alpha'\,\delta\alpha_s' &= 0 \\ \delta\bar{R}_s\sin\beta + \bar{R}\cos\beta\,\delta\beta_s + \frac{\delta\bar{Q}}{2} &= 0. \end{aligned} \tag{28a,b}$$

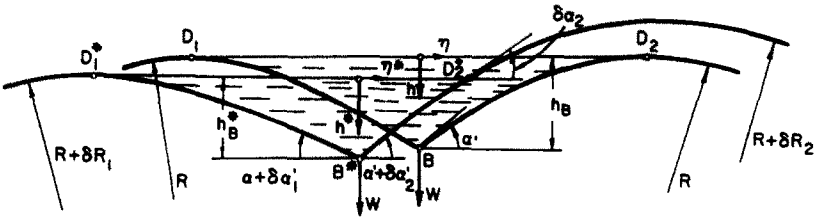

Fig. 3. Laterally disturbed state.

Subtracting and adding eqns (17a) and (17b), and substituting eqn (26) into the resulting relations, one arrives at

$$\delta\bar{R}_a(\pi-\beta)-\bar{R}\,\delta\beta_a-\bar{R}\frac{\delta\alpha_a}{2}+\frac{\delta\bar{L}_1-\delta\bar{L}_2}{2}=0$$

$$\delta\bar{R}_s(\pi-\beta)-\bar{R}\,\delta\beta_s+\bar{R}\frac{\delta\alpha_a}{2}+\frac{\delta\bar{L}_1+\delta\bar{L}_2}{2}=0. \tag{29a,b}$$

Finally, eqns (10), when written in variational form, read

$$\delta\bar{R}_a+\bar{R}\cdot\tfrac{1}{2}\sin\alpha_2\,\delta\alpha_a=0$$

$$\delta\bar{h}_B(1-\bar{h}_B\bar{\gamma})=\delta\bar{R}_s(1-\cos\alpha')+\bar{R}\sin\alpha'\,\delta\alpha'_s+\delta\bar{R}_a. \tag{30a,b}$$

Care needs to be exercised in treating the variation $\delta\alpha_2=\delta\alpha_a$. Clearly, if $\alpha_2=\alpha=0$, which is a requirement for analyzing the structure in the vicinity of the symmetric deformed state, eqn (30a) would seem to lead to $\delta\bar{R}_a=0$, with all other antisymmetric disturbances vanishing. This, in turn, suggests, incorrectly, that no lateral instability is possible. Upon reflection and after examination of this problem, it becomes clear that $\lim_{\alpha_2\to 0}(\sin\alpha_2\,\delta\alpha_a)=(1/2)(\delta\alpha_a)^2$ and $\delta\alpha_a=2\sqrt{(-\delta\bar{R}_a)}$, indicating that any antisymmetric disturbance leads to a negative change in $\delta\bar{R}_a$. Furthermore, the change in $\delta\alpha_a$ will be an order of magnitude higher than the change in $\delta\bar{R}_a$ or a corresponding antisymmetric quantity linearly dependent on $\delta\bar{R}_a$.

Variations of the parameters $\bar{Q}$, $\bar{L}_1$ and $\bar{L}_2$, also appearing in eqns (27)–(30), are expressed in terms of variations of the components of δV as

$$\delta\bar{Q}=\frac{2}{1-\bar{\gamma}\bar{h}_B}\left\{\delta\bar{R}_s\left[\left(\frac{1-\cos\alpha'}{\sin\alpha'}\right)+\frac{H_1}{\bar{R}}(1-\bar{\gamma}\bar{h}_B)\right]+\bar{\gamma}\bar{h}_B\bar{R}\,\delta\alpha_s\right\} \tag{31a}$$

$$\delta\bar{L}_1=\delta\bar{L}_s+\delta\bar{L}_a;\qquad \delta\bar{L}_2=\delta\bar{L}_s-\delta\bar{L}_a-\bar{R}\delta\alpha_a \tag{31b,c}$$

where

$$\delta\bar{L}_s=\delta\bar{R}_s\left(\frac{1}{1-\bar{\gamma}\bar{h}_B}\cdot\frac{1-\cos\alpha'}{\sin\alpha'}+\frac{H}{\bar{R}}\right)+\frac{\bar{R}}{(1-\bar{\gamma}\bar{h}_B)}\cdot\delta\alpha'_a \tag{32a}$$

$$\delta\bar{L}_a=\delta\bar{R}_a\left(\frac{1}{1-\bar{\gamma}\bar{h}_B}\cdot\frac{1-\cos\alpha'}{\sin\alpha'}+\frac{H}{\bar{R}}\right)+\frac{\bar{R}}{1-\bar{\gamma}\bar{h}_B}\,\delta\alpha'_a \tag{32b}$$

$$H=\int_0^{\bar{L}}\frac{\cos\alpha}{1+\cos\alpha}\,\mathrm{d}\bar{L};\qquad H_1=\int_0^{\bar{L}}\frac{\mathrm{d}\bar{L}}{1+\cos\alpha}. \tag{32c,d}$$

Substituting eqns (31) and (32) into eqns (28)–(30), the variation $\delta\alpha_a$ can be eliminated to write the general equation, eqn (23), defining the stability of the system, in the following matrix form

$$\left.\frac{\partial G}{\partial V}\right|_{V=V}\delta V=\left[\begin{array}{c|c} M_L & 0 \\ \hline 0 & M_V \end{array}\right]\cdot\left[\begin{array}{c} \delta\alpha'_a \\ \delta\beta'_a \\ \delta\bar{R}_a \\ \hline \delta\alpha'_s \\ \delta\beta'_s \\ \delta\bar{R}_s \end{array}\right]=0 \tag{33}$$

in which

$$M_L = \begin{bmatrix} -\bar{R}\sin\alpha' & 0 & \cos\alpha' \\ 0 & -\bar{R}\sin\beta & \cos\beta \\ \bar{R} & -(1-\bar{\gamma}\bar{h}_B)\bar{R} & K_1 \end{bmatrix}; \tag{34a}$$

$$M_v = \begin{bmatrix} R\cos\alpha' & 0 & \sin\alpha' \\ \bar{\gamma}\bar{h}_B\bar{R} & (1-\bar{\gamma}\bar{h}_B)\bar{R}\cos\beta & K_2 \\ \bar{R} & -\bar{R}(1-\bar{\gamma}\bar{h}_B) & K_1 \end{bmatrix}; \tag{34b}$$

and where

$$K_1 = \left(\pi-\beta+\frac{H}{\bar{R}}\right)(1-\bar{\gamma}\bar{h}_B)+\frac{\sin\alpha'}{1+\cos\alpha'}$$

$$K_2 = (1-\bar{\gamma}\bar{h}_B)\left(\sin\beta+\frac{H_1}{\bar{R}}\right)+\frac{\sin\alpha'}{1+\cos\alpha'}.$$

It is obvious that eqn (33) represents two separate equations, namely

$$M_L\cdot\delta V_a = 0; \qquad M_v\cdot\delta V_s = 0 \tag{35a,b}$$

in which the first contains only antisymmetric disturbances, δV_a, associated with the lateral buckling of the structure, while the second one refers to the vertical neutral equilibrium state involving only symmetric disturbances, δV_s.

The critical values of the parameters associated with the lateral instability of the structure are obtained from

$$m_L = |M_L| = \bar{R}^2\left\{(1-\bar{\gamma}\bar{h}_B)\sin\alpha'\left[\left(\pi-\beta+\frac{H}{\bar{R}}\right)\sin\beta-\cos\beta\right]+\sin\beta\right\} = 0 \tag{36}$$

while for vertical instability, the corresponding relation reads

$$m_v = |M_v| = \bar{R}^2(1-\bar{\gamma}\bar{h}_B)\cdot[\cos\alpha'(K_2+K_1\cos\beta)-\sin\alpha'(\bar{\gamma}\bar{h}_B+\cos\beta)]. \tag{37}$$

For $\bar{\gamma} = 0$, these equations can be shown to be identical with those presented in Ref. [5] for the case of a symmetric 'line-load-only' applied to the inflatable. To determine critical magnitudes of parameters for lateral or vertical instability, one has to solve, simultaneously, eqn (24a) (defining the symmetric deformation field) with eqn (36) or eqn (37), respectively.

5. NUMERICAL RESULTS

The initial geometry of the structure is defined by θ_0, R_0 and the given load parameters p and γ. The value of the line load W is calculated for every assumed value of the pond depth h_B. The stability of the configuration corresponding to the assumed value of h_B is checked by means of eqns (36) and (37).

Calculations were carried out for the full range of θ_0 values, varying from very high profile structures ($\theta_0 \to 0$) to very flat profile structures with $\theta_0 \to 180°$. The key parameters are conveniently combined into one non-dimensional variable, $\bar{\gamma}$, defined above. In practice, one would normally encounter ponding medium densities of the order of $10^4\ \mathrm{N\,m^{-3}}$ with initial radii and internal overpressure values ranging from $R_0 \simeq 1.0$ to 100 m and $p \simeq 100$ to 1000 Pa, respectively. These values lead to $\bar{\gamma} \cong 10$–10,000. Our analysis covers the range $1.0 \leqslant \bar{\gamma} \leqslant 10{,}000$.

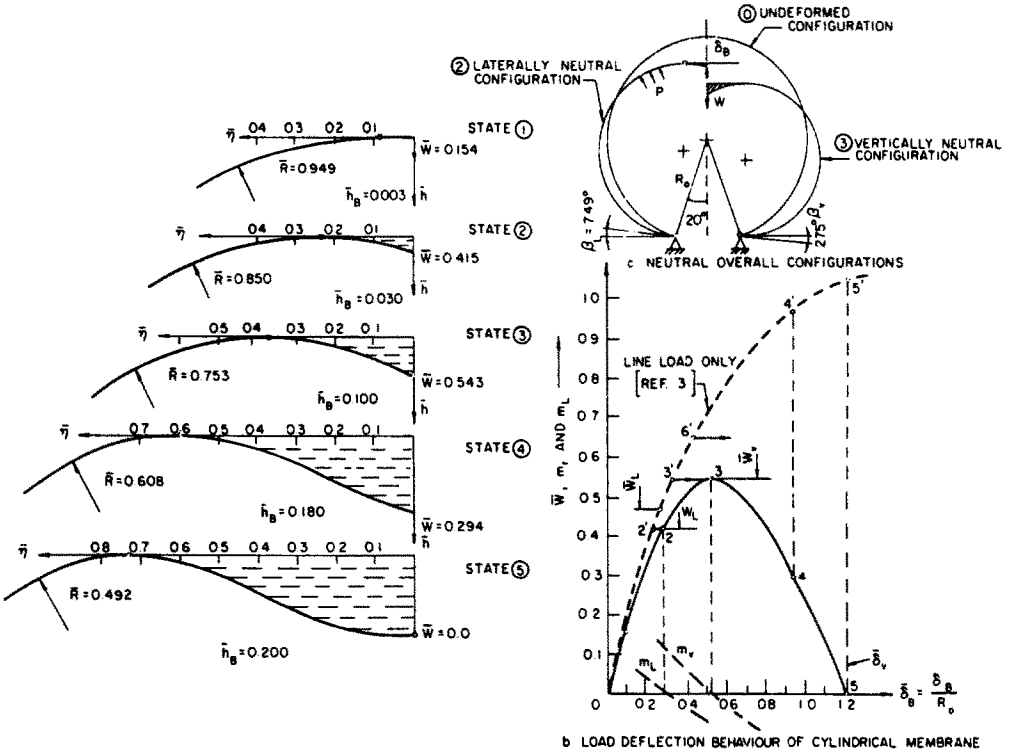

Fig. 4. Load–deflection characteristics of cylindrical membranes.

In order to facilitate the numerical work it might be noteworthy to point out that the depth of the pond can vary from $\bar{h}_B = 0$, for which $\alpha' = \bar{W} = 0$, through $0 < \bar{h}_B < 2/\bar{\gamma}$, over which range $\alpha' > 0$ and $\bar{W} > 0$, up to $\bar{h}_B = \bar{H}_{max} = 2/\bar{\gamma}$, for which value α' and $\bar{W}$ again vanish. This latter configuration corresponds to the critical 'liquid-loading-only' case (see Fig. 1(b), Phase 3). Note also that for $\bar{h}_B = 1/\bar{\gamma}$, using eqn (37) one obtains $m_v = 0$, and consequently $\bar{W}$ takes on an extremum, $\bar{W}_{extr}$. By means of numerical results we demonstrate that this extremum is a 'maximum', referred to in this paper as the vertical critical line load value, $\bar{W}_v$. Analyzing the problem over the full range of $\bar{h}_B$ ($0 < \bar{h}_B \leqslant \bar{H}_{max}$) one determines the characteristic load/deflection features of such membrane structures.

Typical results from such an analysis are given in Fig. 4 where consecutive configurations of the deformed shapes, for $\bar{\gamma} = 10$ and $\theta_0 = 20°$, are given in Fig. 4(a). The central deflection $\bar{\delta}_B$, is monotonically increasing with $\bar{h}_B$, while $\bar{W}$ increases only up to its maximum value, $\bar{W}_v$, for which $\bar{h}_B = 1/\bar{\gamma} = 0.1$; from there on, $\bar{W}$ decreases until $\bar{h}_B = 2/\bar{\gamma} = 0.2$, for which case $\bar{W} = 0$. A plot of $\bar{W}$, as well as m_L and m_v, vs the non-dimensionalized deflection, $\bar{\delta}_B$, is given in Fig. 4(b) where the corresponding load/deflection curve for the line-load-only case is indicated by means of the dashed curve and is taken from Ref. [5]. Lateral instability occurs at a line-load value, $\bar{W} = \bar{W}_L$, determined from the relation $m_L = 0$. The corresponding point on the load–deflection diagram is designated as point 2, with the associated neutral configuration of the whole cross-section shown in Fig. 4(c) (Configuration (2)). Note also from Fig. 4(c) that the value of β for this case is given as $\beta_L = 7.49°$, which for all examples used in the analysis was found to be greater than zero. Thus, in these cases, a possible horizontal surface adjacent to the supports would not influence the lateral stability of the structures, a conclusion similar to that reached in Ref. [5] for the 'line-load-only' case. Note that the value of $\bar{W}_L$ in the presence of a ponding medium is lower than the corresponding value for the 'line-load-only' loading case.

The only meaningful solution of the stability equation $m_v = 0$ is found for $\bar{h}_B = 1/\bar{\gamma}$ and corresponds to $\bar{W} = \bar{W}_v$, the maximum value of the line load, denoted as point 3 on Fig. 4(b). The corresponding neutral configuration, with $\beta_v = -2.75°$, is also indicated on Fig. 4(c). For line load values, $\bar{W} \leqslant \bar{W}_v$, the increment in central deflection caused by the ponding medium is given by the horizontal distance between the two curves on Fig. 4(b), lines such as $2' \to 2$, or $3' \to 3$.

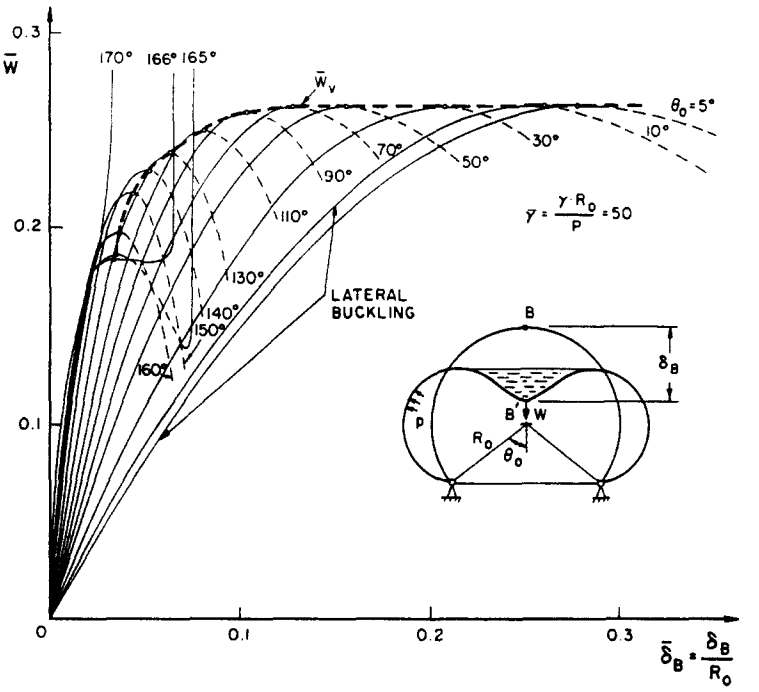

Fig. 5. Load–deflection and stability behaviour of symmetrically deformed cylindrical membrane.

The descending portion of the curve for $\bar{W}$ in the presence of a ponding medium, naturally, represents unstable equilibrium for an 'active' line load of fixed magnitude. For the 'passive' line load case, with fixed deflection and caused by tie-downs, this portion of the curve still denotes stable configurations. In fact, the difference in ordinate between the two curves, such as the distance between points 4–4', represents the reduction in tension in the tie-down cables due to the accumulating ponding medium. The maximum value of such reduction is indicated by the vertical line 5–5' and is associated with the maximum 'critical' value of the central deflection, $\bar{\delta}_v$. Thus $\bar{\delta}_v$ represents the limiting initial central deflection for which the accumulation process terminates, implying a stable structure.

Curves similar to the one obtained for $\bar{\gamma} = 10$ and $\theta_0 = 20°$, and shown on Fig. 4(b), can be drawn for various fixed values of these parameters. For example, Fig. 5 indicates a family of such curves for $\bar{\gamma} = 50$ and for a full range of θ_0 values. It shows the variation of the maximum value of the line loads, $\bar{W}_v$, with θ_0 by means of a dashed curve connecting the maximum of each of the individual load/deflection curves. It also shows that there is no maximum for load/deflection curves of structures for which $\theta_0 \gtrsim 166°$; thus no vertical instability is possible, in the presence of a ponding medium, for extremely flat profiled membranes. The load/deflection curves for $5° < \theta_0 < 160°$ are very similar in overall appearance and characteristics. Values of the line load at which lateral instability is imminent, designated by $\bar{W}_L$, are shown on this figure only for $\theta_0 = 5°$ and 10°. In fact, it can be shown that for $\bar{\gamma} = 50$, no lateral instability is possible for structures with a central half angle, $\theta_0 \gtrsim 11.8°$.

As one can observe from both Figs 5 and 6, the critical value of the line load for vertical stability, $\bar{W}_v$, is nearly constant over the range $0 < \theta_0 \leqslant 90°$. For greater values of this parameter, i.e. for lower profile structures, $\bar{W}_v$ decreases slightly. Figure 6 shows also the variation of $\bar{W}_L$ for the relatively small range of $0 < \theta_0 \leqslant 11.8°$. In fact the whole critical load domain shown on this figure consists of three main areas: (i) the domain of possible lateral instability ($\theta_0 \leqslant 11.8°$); (ii) the domain of possible vertical instability ($11.8° < \theta_0 \lesssim 166°$); (iii) a stable domain ($166° \lesssim \theta_0 < 180°$). These domains and their respective boundaries are very sensitive to changes in the value of $\bar{\gamma}$. Carrying out analogous analyses for other fixed values of $\bar{\gamma}$ one obtains a family of such curves shown on Fig. 7 which indicate that with increasing $\bar{\gamma}$ the range of the vertical instability domain expands, in both directions, while, at the same time, the value of $\bar{W}_v$ decreases. The range in $\bar{W}_v$, as denoted by the difference $\bar{W}'_v - \bar{W}''_v$ (see

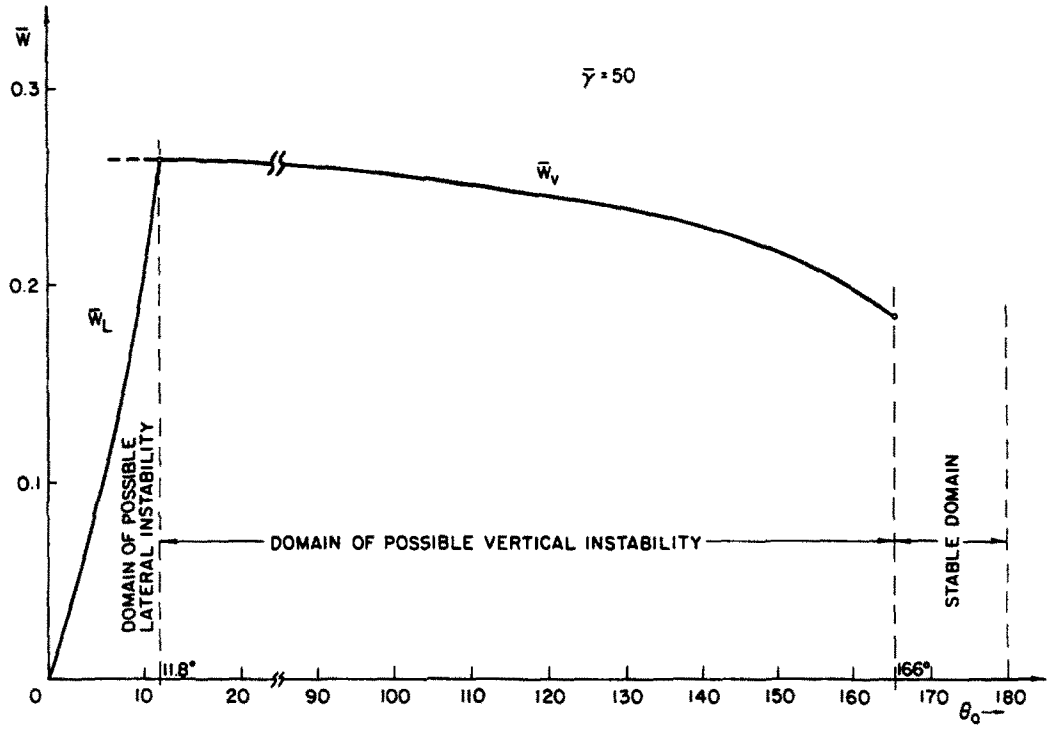

Fig. 6. Stability domains of cylindrical inflatable loaded by uniform line load and ponding medium.

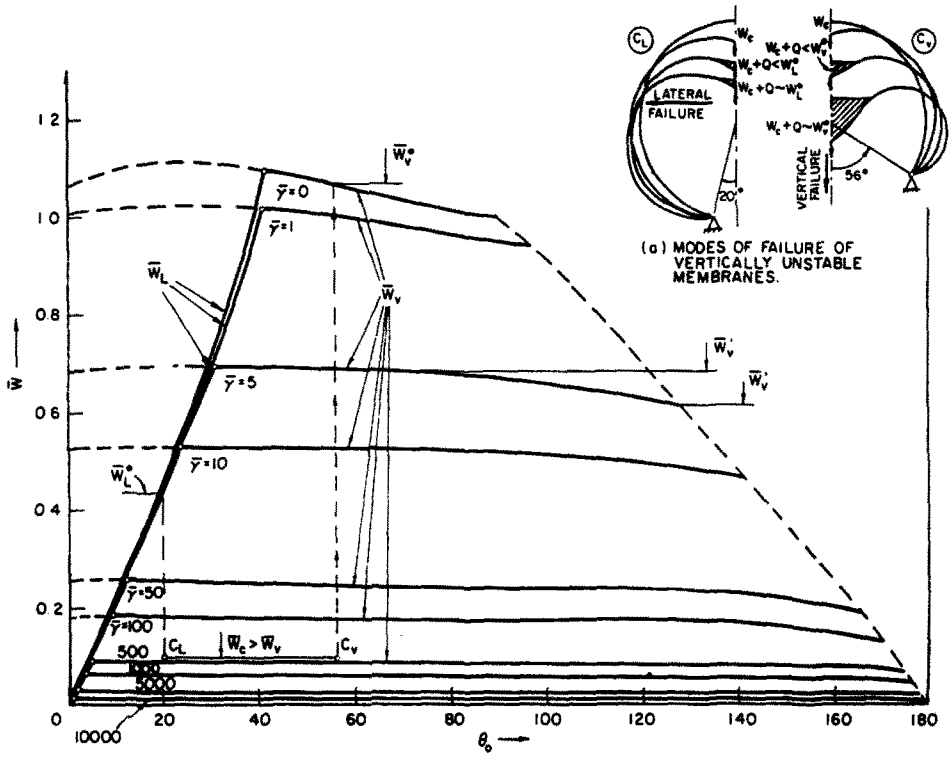

Fig. 7. Variation of stability domains of cylindrical inflatables with $\bar{\gamma}$.

Fig. 7) decreases with increasing $\bar{\gamma}$; i.e. for high $\bar{\gamma}$ values, say $\bar{\gamma} > 50$, $\bar{W}_V$ is practically constant for all profiles of such membranes. This, in turn suggests that $\bar{W}_V$ is approximately independent of θ_0 and is a function only of $\bar{\gamma}$.

What might be surprising at first from these results is the indication that vertical instability is the governing mode of failure even for very high profiled membranes, structures for which one might intuitively look for lateral instability phenomena. Upon reflection and

analyzing the exact nature of the loading one easily reconciles this apparent contradiction. Consider, for example, two cylindrical membrane structures with $\bar{\gamma} = 500$ and $\theta_0 = 20°$ and 56°, respectively. Assume that the line load value, $\bar{W}_c$, exceeds the critical load, $\bar{W}_c > \bar{W}_v$ (see points C_L and C_v on Fig. 7). Due to the inherent vertical instability in such a loading configuration, the weight of the pond, Q, will be monotonically increasing up to a certain value. In the case of the higher profile structure ($\theta_0 = 20°$) this unstable accumulation process continues till the total load approaches the value $\bar{W}_L$ for the corresponding 'line-load-only' case at which time the structure collapses dynamically laterally. For the $\theta_0 = 56°$ geometry, the pond weight, Q, will grow until the total load reaches the value $\bar{W}_v$ for the corresponding 'line-load-only' case at which instance the final vertical dynamic collapse process initiates. In both cases the underlying real reason for the collapse was the inherent vertical instability due to the value $\bar{W}_c > \bar{W}_v$.

Interestingly, when one plots $\bar{W}'_v$ and $\bar{W}''_v$ as a function of $\bar{\gamma}$ to a log–log scale, as is done on Fig. 8, one finds that over the range $10 \gtrsim \bar{\gamma} < 100{,}000$, these plots are approximately straight lines. Therefore one can describe such a relation by means of a relatively simple expression written as

$$\bar{W}_v \cong \frac{1.63}{\bar{\gamma}^{0.47}} \tag{38a,b}$$

or

$$W_v = \frac{1.63 R_0^{0.53} p^{1.47}}{\gamma^{0.47}}.$$

Experimental results on the ponding instability for cylindrical inflatables undergoing relatively small deflections, reported in Refs [5, 9], are also indicated on Fig. 8 and show excellent agreement with our analytical predictions.

The critical initial central deflection, $\bar{\delta}_v$, as defined on Figs 1(b) and 4(b), is determined by assuming $\bar{h}_B = 2/\bar{\gamma}$ for which $\alpha' = 0$ and $\bar{W} = 0$. Such a configuration subjected only to hydrostatic pressure loading can be checked for lateral instability by means of eqn (36) which for this case reduces to

$$m_L = \bar{R}^2 \sin\beta = 0 \tag{39}$$

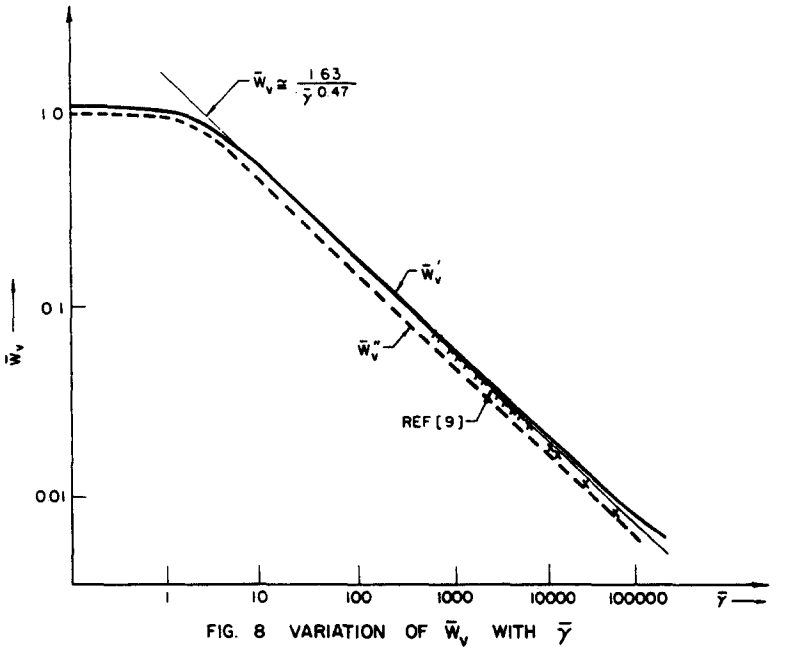

FIG. 8 VARIATION OF $\bar{W}_v$ WITH $\bar{\gamma}$

Fig. 8. Variation of $\bar{W}_v$ with $\bar{\gamma}$.

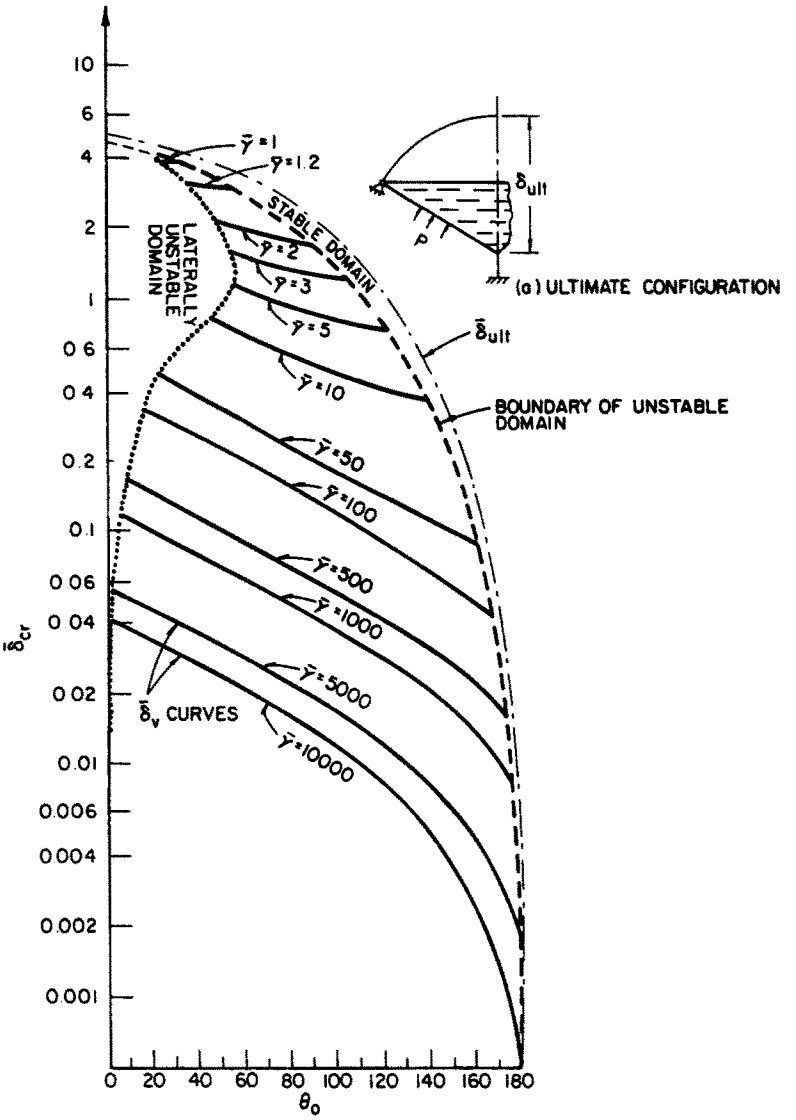

Fig. 9. Variation of critical initial central deflection with θ_0 for various values of $\bar{\gamma}$.

and yields a very simple condition for bifurcation, namely $\beta = 0$. The configuration satisfying this criterion is characterized by the deflection parameter $\bar{\delta}_L$ referred to here as the 'laterally critical initial central' deflection. Figure 9 shows variations of $\bar{\delta}_v$ and $\bar{\delta}_L$ as functions of θ_0 for various values of $\bar{\gamma}$. It indicates that lateral instability is a possible mode of failure only for very high profile membranes with values of $\bar{\gamma} \gtrsim 50$ and for moderately high profile structures for the density range $2 \lesssim \bar{\gamma} \lesssim 10$. For the latter range, $\bar{\delta}_v$ and $\bar{\delta}_L$ are very large, comparable to or exceeding the initial rise of the structure. Note that on this figure $\bar{\delta}_v$ curves are given as solid lines while the single $\bar{\delta}_L$ curve is dotted. There may be initial geometry and density combinations for which no critical initial central deflection can be obtained; i.e. for such a configuration, any initial central deflection, $0 < \bar{\delta} < \bar{\delta}_{ult}$ results in a non-zero tension in the tie-down cables with the pond filling the depression to capacity. These configurations are indicated by the dashed line on Fig. 9. The area between this line and the line denoting the ultimate deflection, $\bar{\delta}_{ult}$ (see Fig. 9(a)) represents the so-called 'stable domain' for the combination of liquid-loading and 'passive' tie-down line load.

The same results are plotted, as a function of $\bar{\gamma}$ and for various constant θ_0 values on Fig. 10. Again, the 'stable domain' boundary is denoted by a dashed line, while the $\bar{\delta}_{ult}$ curve of Fig. 9 becomes a series of horizontal lines on this figure. The $\bar{\delta}_v$ curves are solid and the $\bar{\delta}_L$ curve is dotted. Note also that the $\bar{\delta}_v$ curves are nearly straight lines on this log–log plot, except for small values of $\bar{\gamma}$, for which $\bar{\delta}_v$ are very large, and for very flat membranes with

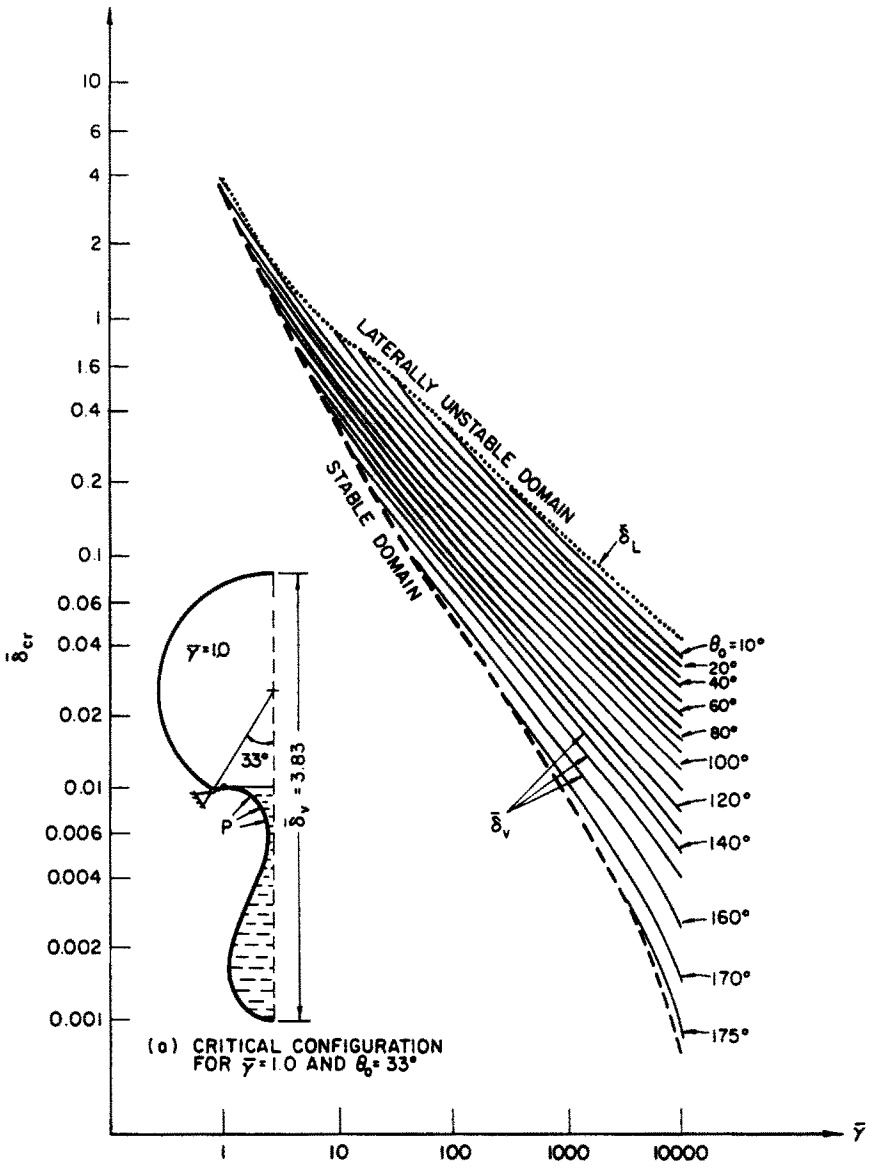

Fig. 10. Variation of critical initial central deflection with $\bar{\gamma}$ for various values of θ_0.

$\theta_0 \to 180°$. Over the larger, central portion of the $\bar{\gamma}$ domain one can therefore represent the dependence of $\bar{\delta}_v$ on $\bar{\gamma}$ by a relatively simple approximate expression in the form

$$\bar{\delta}_v = \frac{C(\theta_0)}{\sqrt{\bar{\gamma}}} \quad \text{or} \quad \delta_v = \sqrt{\left(\frac{R_0 p}{\gamma}\right)} C(\theta_0) \tag{40}$$

where $C(\theta_0) = 10^x$ with $x = 0.65 - 0.006\ \theta_0$ and θ_0 in degrees. Equations (30) and (40) provide relatively simple expressions for the designer to estimate the critical value of the line load and the magnitude of the critical initial central deflection for such cylindrical inflatables.

6. CONCLUSIONS

The results obtained from an 'exact' analysis of the large deflection and stability behaviour of cylindrical inflatables subjected to symmetric line loads in the presence of an accumulating ponding medium show that ponding instability may occur for nearly every shape of such structures, including very high profile and very flat membranes. Ponding instability is very important for the designer especially in the case of large structures

operating under relatively low inflation pressures in which cases critical line load values or critical initial central deflection magnitudes are relatively small and may therefore be easily exceeded during the operational lifetime of the structure.

Excluding unusual designs, cylindrical geometries for such structures are normally such as to make vertical instability the governing mode of failure placing limits on allowable 'safe' line load values or initial central deflections/imperfections.

The results also show that the critical 'active' line load value for vertical instability, $\bar{W}_v$, is nearly independent of the initial central half angle, θ_0, indicating this problem to be of a 'local' nature and largely unaffected by the support conditions of the membrane. Simple approximate expressions for $\bar{W}_v$ and the critical initial central deflection, $\bar{\delta}_v$, as functions of $\bar{\gamma}$, are given and should be useful during the proper design of such inflatables. They may also be convenient for inclusion in possible codes/standards for this class of structures.

Acknowledgements—The results presented here were obtained in the course of research sponsored by the Natural Sciences and Engineering Research Council of Canada, Grant No. A-2736.

REFERENCES

1. H. Megara, K. Okamura and M. Kawaguchi, An analysis of membrane structures. *Shell and Spatial Structures Engineering—Proc. of I.A.S.S. Symposium*, Rio de Janeiro, pp. 1–12 (1983).
2. K. Ishii, Structural design of cable-reinforced membrane structure. *Shell and Spatial Structures Engineering—Proc. of I.A.S.S. Symposium*, Rio de Janeiro, pp. 56–76 (1983).
3. P. G. Glockner and W. Szyszkowski, Some stability considerations of inflatable structures. *Shell and Spatial Structures Engineering—Proc. of I.A.S.S. Symposium*, Rio de Janeiro, pp. 116–134 (1983).
4. D. J. Malcolm and P. G. Glockner, Collapse by ponding of air-supported spherical caps. *Proc. ASCE* **104**(ST9), 1731–1742 (1981).
5. D. J. Malcolm and P. G. Glockner, Collapse by ponding of air-supported membranes. *Proc. ASCE* **104**(ST9), 1525–1532 (1978).
6. W. Szyszkowski, S. Lukasiewicz and P. G. Glockner, Lateral stability of symmetrically loaded cylindrical inflatables. *Spatial Roof Structures, Proc. of I.A.S.S. Symposium*, Dortmund, pp. 1.3.051–082 (1984).
7. S. Lukasiewicz and P. G. Glockner, Ponding instability of cylindrical air-supported membranes under non-symmetrical loadings. Dept. of Mech. Engng Report No. 205, University of Calgary, Calgary, Alberta, Canada (June 1981).
8. A. S. Volmir, *Stability of Deformable Systems*. Nauka, Moskow (1967), in Russian.
9. D. J. Malcolm, Ponding instability of air-supported cylinders—some experimental results. Dept. of Mech. Engng Report No. 132, University of Calgary, Calgary, Alberta, Canada (December 1978).